

Orientational Phase Transition in the System Pyridine/Ag(111): A Near-Edge X-Ray-Absorption Fine-Structure Study

M. Bader, J. Haase, K.-H. Frank, and A. Puschmann

Fritz-Haber-Institut der Max-Planck-Gesellschaft, D-1000 Berlin 33, West Germany

and

A. Otto

Physikalisches Institut, Universität Düsseldorf, D-4000 Düsseldorf 1, West Germany

(Received 20 February 1986)

A phase transition has been observed in the system pyridine adsorbed on Ag(111) at 100 K by near-edge x-ray-absorption fine-structure measurements in real time. At low pyridine coverages an angle between the ring plane and the surface plane of $45^\circ \pm 5^\circ$ was observed. This phase converts sharply at a submonolayer coverage to a phase with an angle between the ring plane and the surface plane of $70^\circ \pm 5^\circ$. Continued exposure gradually leads to a randomly oriented multilayer.

PACS numbers: 68.35.Rh, 68.35.Bs, 78.70.Dm

There is widespread interest in the pyridine-silver system because of its importance for surface-enhanced Raman scattering.¹⁻³ In particular, some proposed enhancement models involve charge-transfer excitations from the metal to affinity levels of the adsorbate,^{4,5} which are also probed by the near-edge x-ray-absorption fine-structure (NEXAFS) technique.⁶⁻⁸ Pyridine (C_5H_5N) is electronically characterized by a nitrogen lone-pair orbital. Pyridine chemisorption on metal surfaces may therefore have model character for determining the relative contributions of lone-pair and π bonding to the chemisorption bond. Here we report the coverage-dependent molecular orientation of pyridine chemisorbed on Ag(111) at 100 K determined by NEXAFS.

Demuth, Christmann, and Sanda⁹ studied the chemisorption of pyridine on clean Ag(111) surfaces at ~ 140 K with vibrational electron-energy-loss (VEELS) and uv-photoemission spectroscopies (UPS). They observed a phase transition at about half a monolayer coverage from a nearly flat-lying π -bonded pyridine phase to an inclined N-bonded phase. Similar coverage-dependent orientational phase transitions have been obtained by VEELS for pyridine on Ni(001)¹⁰ and Pt(110).¹¹ Orientational phase transitions also occur as a function of temperature. This has been shown for pyridine on Ni(001) by VEELS¹⁰ and for pyridine on Pt(111) in a recent NEXAFS study.¹² The NEXAFS measurements on Pt(111) indicated a low-temperature pyridine state with an apparent angle between the ring plane and the surface plane of 52° which converts at $T \leq 300$ K to a high-temperature state with a corresponding tilt angle of 74° . This result, as well as UPS and electronic EELS data for pyridine on Ag(111),^{13,14} casts some doubt on the existence of flat-lying pyridine molecules on well-defined surfaces at low coverages.

NEXAFS studies on molecules which are only weak-

ly perturbed by chemisorption are particularly useful in determining the orientation of the molecules relative to the surface.⁶⁻⁸ For low-symmetry surfaces this includes the determination of the azimuthal orientation.¹⁵ The polarization dependence of NEXAFS transitions is due to the validity of dipole selection rules for photoabsorption. The analysis of NEXAFS is especially unambiguous when π resonances occur resulting from transitions of a $1s$ electron into unfilled antibonding π states. These π resonances are rather sharp compared with σ shape resonances so that background subtraction is straightforward. With high-brightness storage rings and the new generation of grazing-incidence monochromators, phase transitions which are characterized by orientational changes can be observed by NEXAFS in real time.

We report here for the first time such a phase transition measured by NEXAFS in real time during continuous adsorption of pyridine on Ag(111) at 100 K. π and σ resonance intensities were analyzed as a function of the angle between the electric field vector E and the surface normal. The analysis of the π intensities proved that at low pyridine coverages the ring plane is tilted by 45° with respect to the surface. Thus even at low coverages nitrogen lone-pair bonding pertains.

The experiments were performed at the Berlin storage ring for synchrotron radiation, BESSY, with the plane-grating grazing-incidence monochromator SX-700¹⁵ with a 1200-lines/mm grating. The data were taken in the partial electron-yield mode⁸ running the monochromator with a sweep rate of 30 eV/min. The spectra shown are background corrected (covered minus clean). The NEXAFS was studied at the C and N K edges. The photon energy was calibrated in this region to an accuracy of ± 0.5 eV. The x-ray incidence angle on the sample could be varied from near grazing incidence ($\theta = 20^\circ$) to normal incidence

($\theta = 90^\circ$). To correct for experimental changes by varying the incidence conditions, exposure and photon-flux resonance intensities were normalized by the height of the underlying atomic adsorption step.⁶ Two types of experiments were conducted: (a) continuous NEXAFS measurements for $\theta = 20^\circ$ and $\theta = 90^\circ$ during exposure with pyridine with an exposure rate of ~ 0.1 L/min [1 L (langmuir) = 10^{-6} Torr sec] and (b) NEXAFS measurements with fixed doses. The Ag(111) crystal, mechanically and chemically polished, was cleaned by Ar⁺ bombardment and subsequent annealing at ~ 600 K. Good $p(1 \times 1)$ LEED patterns were obtained. During exposure and measurement the Ag(111) crystal was held at a temperature of ~ 100 K.

Characteristic N *K*-edge NEXAFS spectra of pyridine on Ag(111) are shown in Fig. 1. The main structures labeled A–D are the same as in benzene NEXAFS spectra.^{16,17} There are two unfilled π^* orbitals in benzene¹⁸ with e_{2u} and b_{2g} symmetry, separated by 3.7 eV, which correspond to peaks A and B, respectively. In pyridine the degenerate e_{2u} orbital is split by 0.6 eV

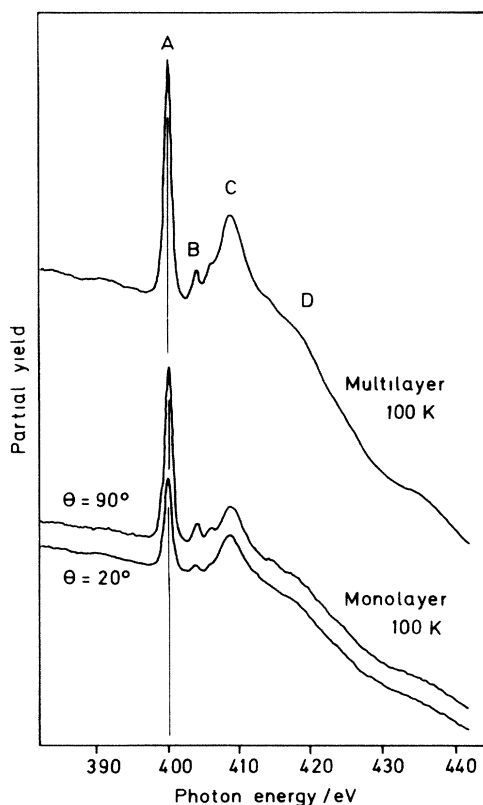


FIG. 1. Nitrogen *K*-edge NEXAFS spectra of condensed multilayers (above) and of a monolayer (below) of pyridine on Ag(111) at 100 K. The monolayer spectra were taken at normal ($\theta = 90^\circ$) and at near grazing ($\theta = 20^\circ$) x-ray incidence. Four main structures labeled A–D are observed. For peak assignment see text.

into two levels of b_1 and a_2 symmetry,¹⁸ which in this experiment were not resolved because the monochromator resolution was set at 1.2 eV (N *K* edge). The measured energy separation between peaks A and B is 3.8 ± 0.2 eV. Peaks A and B show the same polarization dependence. In the remainder of the paper we will analyze only peak A and refer to it as the “ π resonance.” There is no disagreement in the literature about the assignment of peak D as σ resonance. In inner-shell EELS measurements of benzene¹⁹ peak C, however, was assumed to be a shakeup structure, whereas recent multiple scattering calculations for benzene¹⁷ suggest that peak C is also a σ resonance.

The results of the real-time NEXAFS experiments and the NEXAFS measurements at fixed doses are shown in Fig. 2. During continuous adsorption of pyridine on Ag(111) the normalized π -resonance intensity for normal incidence, I_{90} , rises drastically between 4 and 5.5 L and steadily decreases at higher doses. A similar π -resonance intensity measurement for near grazing incidence ($\theta = 20^\circ$) enabled us to plot the ratio I_{20}/I_{90} as a function of dose. I_{20}/I_{90} also changes drastically in the same dose range. Measurements of the intensity ratio I_{20}/I_{90} at fixed doses between ~ 0.8 and 15 L (multilayer) fit the latter curve perfectly. As the π -resonance intensity ratio measures the tilt angle α between the ring plane and the surface (see below), the results indicate a phase transition characterized by an orientational change of the pyridine molecules on the Ag(111) surface as a function of coverage.

The ring plane of pyridine is a nodal plane for the π orbitals in this molecule.²⁰ As the π -resonance intensity varies with $\cos^2\gamma$, where γ is the angle between the vector **E** and the normal to the nodal plane,⁶ we can calculate the π -resonance intensity I_π as a function of the polar angle θ and of the tilt angle α between the surface normal and the normal to the ring plane. If we assume rotational symmetry,¹² the following expression for radiation with a degree of linear polarization P holds:

$$I_\pi \propto [P(\sin^2\alpha \sin^2\theta + 2\cos^2\alpha \cos^2\theta) + (1-P)\sin^2\alpha]. \quad (1)$$

NEXAFS measurements at fixed doses before (2.3 L) and after (5.3 L) the phase transitions are shown in Fig. 3. Fits (full lines) according to Eq. (1) with²¹ $P = 0.87$ yield tilt angles of $\alpha = 45^\circ \pm 5^\circ$ at 2.3 L and $\alpha = 70^\circ \pm 5^\circ$ at 5.3 L. Comparing these results with the data in Fig. 2 we see that at low pyridine coverages a constant angle between the ring plane and the surface of $\alpha = 45^\circ$ is measured. This state converts between about 4 and 5.5 L to a state with approximately $\alpha = 70^\circ$. Around 5.5 L the intensity ratio I_{20}/I_{90} has a minimum. Continued exposure results in gradually

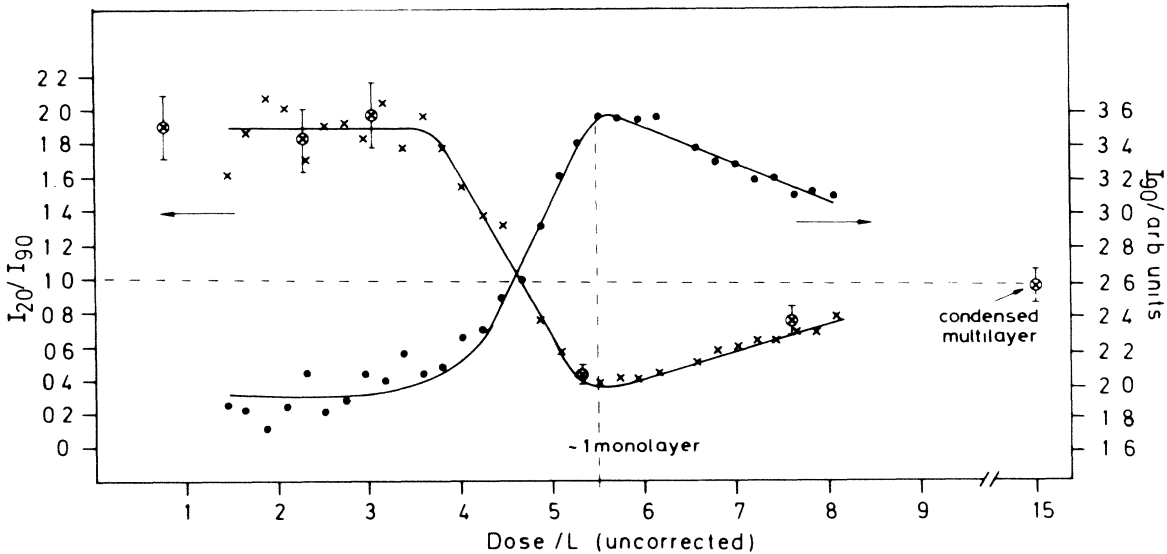


FIG. 2. Normalized nitrogen K -edge π -resonance (peak A) intensity for normal incidence ($\theta = 90^\circ$), I_{90} (full circles), and the intensity ratio I_{20}/I_{90} (crosses) as a function of dose during permanent adsorption of pyridine (~ 0.1 L/min) on Ag(111) at 100 K. The I_{20}/I_{90} data points with error bars were independently measured at fixed pyridine doses. There is a phase transition near 4.5 L.

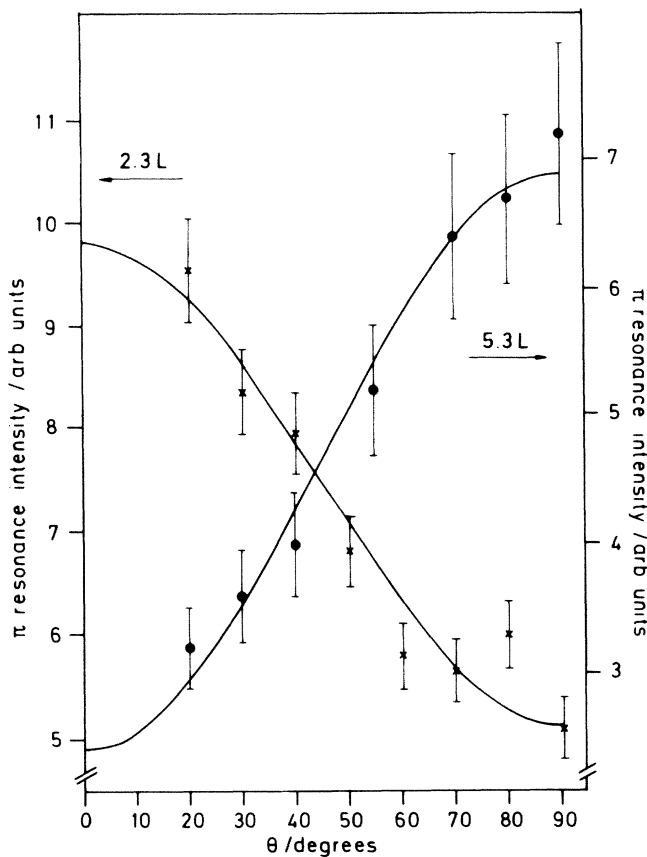


FIG. 3. Nitrogen K -edge π -resonance intensity (peak A) for submonolayer coverages (2.3 and 5.3 L) of pyridine on Ag(111) at 100 K as a function of the angle of incidence, θ . The full lines are least-squares fits according to Eq. (1) which yield tilt angles of 45° and 70° , respectively.

increasing values, which finally approach $I_{20}/I_{90} = 1$ for a randomly oriented condensed multilayer. We therefore assign a monolayer to an exposure of approximately 5.5 L. This is in good agreement with inverse photoemission spectroscopy, UPS, and work-function results¹³ which indicate a monolayer coverage for 4.6- to 5.8-L exposure. The phase transition is thus observed for a submonolayer coverage in agreement with the VEELS data.⁹

The measured tilt angles are apparent angles between the molecular plane and the surface plane. They could result from a single phase or a number of coexistent phases with well-defined tilt angles. But they could also result from a phase with pyridine molecules rotated around their symmetry axis which has a well-defined inclination angle with respect to the surface ("rotated" model). For the apparent angle of $\alpha = 70^\circ$ all explanations are possible; in the rotated model the inclination angle would then be 41° . An apparent angle of $\alpha = 45^\circ$, however, would correspond to an inclination angle of 0, which is physically unreasonable. For $\alpha = 45^\circ$ the rotated model thus cannot be appropriate.

The intensities of peaks C and D (σ shape resonance) proved to be constant within $\pm 15\%$ for all measured polar angles θ at low and high pyridine coverages. A comparison with the strongly varying σ -resonance intensity of the flat-lying benzene on Cu(110) and with the weak intensity variation of the upright standing pyridine on Cu(110)¹⁶ indicates that the measured tilt angle of 45° for pyridine on Ag(111) cannot be due to a "mixture" of flat-lying and nearly perpendicularly oriented molecules.

The measured tilt angles for pyridine on Ag(111) compare well with those found by NEXAFS for pyridine on Pt(111).¹² Moreover, a recent electron-stimulated-desorption ion angular distributions study of pyridine adsorbed on Ir(111) at room temperature²² indicated an angle between the ring plane and the surface of 70° in agreement with the NEXAFS results mentioned above.

The measured tilt angle for the low-coverage, low-temperature phase of pyridine on Ag(111) of 45° is at variance with that indicated by VEELS for pyridine on Ag(111)⁹ and Ni(001),¹⁰ where nearly flat-lying molecules are suggested. This means that even for the same system [pyridine/Ag(111)] there is a strong discrepancy between VEELS and NEXAFS results.

VEELS can determine molecular orientations via selection rules only if dipole scattering dominates, which is not always the case.²³ For the systems pyridine on Ag(111) and Ni(001) it has been shown by measuring both on and off specular that dipole scattering dominates for some major spectral features. But even then exact tilt angles could not be calculated because of the dependence of the dynamic dipole moment on the orientation of the molecule relative to the surface.¹⁰ Further careful VEELS and NEXAFS studies on identical systems should help to solve the obvious discrepancies.

In summary, our NEXAFS results show clearly the existence of a phase transition at a submonolayer coverage in the system pyridine/Ag(111) at 100 K. At low coverage the ring plane of the pyridine molecules is tilted by 45° with respect to the surface in contrast to VEELS results which seem to indicate nearly flat-lying molecules. Our NEXAFS results suggest, therefore, that even at low coverages N lone-pair bonding occurs. At saturation coverage the pyridine molecules are nearly perpendicularly oriented or rotated around their symmetry axis which is inclined by 41° with respect to the surface. It has been shown that NEXAFS can detect orientational phase transitions in real time.

The authors are pleased to acknowledge the support of the Bundesministerium für Forschung und Technologie under Grant No. 05238 JH. We thank E. E.

Koch for providing the Ag(111) crystal.

¹R. K. Chang and T. E. Furtak, *Surface Enhanced Raman Scattering* (Plenum, New York, 1982).

²A. Otto, in *Light Scattering in Solids*, edited by M. Cardona and G. Güntherodt (Springer, Berlin, 1984), Vol. 4.

³I. Pockrand, *Surface Enhanced Raman Vibrational Studies at Solid/Gas Interfaces*, Springer Tracts in Modern Physics Vol. 104 (Springer, New York, 1984).

⁴A. Otto, J. Billmann, J. Eickmans, Ü. Estürk, and C. Pettenkofer, *Surf. Sci.* **138**, 319 (1984).

⁵J. Thietke, J. Billmann, and A. Otto, in *Dynamics on Surfaces*, edited by B. Pullmann *et al.* (Reidel, Dordrecht, 1984).

⁶J. Stöhr and R. Jaeger, *Phys. Rev. B* **26**, 4111 (1982).

⁷J. Stöhr, in *X-Ray Absorption: Principles, Applications, Techniques of EXAFS, SEXAFS and XANES*, edited by R. Prins and D. Koningsberger (Wiley, New York, 1985).

⁸J. Haase, *Appl. Phys. A* **38**, 181 (1985).

⁹J. E. Demuth, K. Christmann, and P. N. Sanda, *Chem. Phys. Lett.* **76**, 201 (1980).

¹⁰N. J. DiNardo, Ph. Avouris, and J. E. Demuth, *J. Chem. Phys.* **81**, 2169 (1984).

¹¹N. V. Richardson, *Vacuum* **33**, 787 (1983).

¹²A. L. Johnson, E. L. Muetterties, J. Stöhr, and F. Sette, *J. Phys. Chem.* **89**, 4071 (1985).

¹³A. Otto, K.-H. Frank, and B. Reihl, *Surf. Sci.* **163**, 140 (1985).

¹⁴R. Dudge, Deutsches Elektronen Synchrotron Report No. DESY F41, 1984 (unpublished).

¹⁵A. Puschmann, J. Haase, M. D. Crapper, C. E. Riley, and D. P. Woodruff, *Phys. Rev. Lett.* **54**, 2250 (1985).

¹⁶M. Bader *et al.*, to be published.

¹⁷J. A. Horsley, J. Stöhr, A. P. Hitchcock, D. C. Newbury, A. L. Johnson, and F. Sette, *J. Chem. Phys.* **83**, 6099 (1985).

¹⁸I. Nenner and G. J. Schulz, *J. Chem. Phys.* **62**, 1747 (1975).

¹⁹A. P. Hitchcock and C. E. Brion, *J. Electron Spectrosc. Relat. Phenom.* **10**, 317 (1977).

²⁰W. L. Jorgensen and L. Salem, *The Organic Chemist's Book of Orbitals* (Academic, New York, 1973).

²¹M. D. Crapper, C. E. Riley, D. P. Woodruff, A. Puschmann, and J. Haase, to be published.

²²J. U. Mack, E. Bertel, and F. P. Netzer, *Surf. Sci.* **159**, 265 (1985).

²³G. L. Nyberg, S. R. Bare, P. Hofmann, D. A. King, and M. Surman, *Appl. Surf. Sci.* **23**, 392 (1985).